Energy Dispersive Extended X-ray Absorption Fine Structure, Mass Spectrometric, and Diffuse Reflectance Infrared Studies of the Interaction of Al_2O_3-Supported $Rh^I(CO)_2Cl$ Species with NO and Re-formation under CO

Mark A. Newton,*,† Daryl G. Burnaby,† Andrew J. Dent,‡ Sofia Diaz-Moreno,§ John Evans,*,† Steven G. Fiddy,† Thomas Neisius,§ and Sandra Turin†

Department of Chemistry, University of Southampton, Highfield, Southampton, U.K. SO17 1BJ, European Synchrotron Radiation Facility, Grenoble F-38043, France, and CLRC Daresbury, Warrington, U.K. WA4 4AD

Received: October 9, 2001; In Final Form: January 31, 2002

The interaction between supported $Rh^I(CO)_2Cl$ species, prepared by metallo-organic chemical vapor deposition (MOCVD) of $[Rh(CO)_2Cl]_2$ to hydroxylated γ-Al_2O_3, and NO has been investigated using time-resolved, energy dispersive extended X-ray absorption fine structure (EDE)/mass spectrometry (MS) and diffuse reflectance infrared Fourier transform spectroscopy (DRIFTS). MOCVD of $[Rh^I(CO)_2Cl]_2$ leads to the formation of a $Rh^I(CO)_2Cl\{O-Al\}$ adlayer which, when fresh, reacts with NO to form a majority $\{Al-O\}_2RhCl(NO^-)$ species at room temperature via a two-step mechanism involving an $\{Al-O\}Rh(NO)_2Cl$ species. The application of DRIFTS allows a direct association of the bent RhNO bonding in the $\{Al-O\}_2RhCl(NO)^-$ with "high-wavenumber" $Rh(NO^-)$ species displaying ν(NO) at ca. 1750 cm^{-1} often observed in supported Rh systems. DRIFTS investigations on analogous $Rh^I(CO)_2Cl/TiO_2$ systems show the same reactivity toward NO, with a bent nitrosyl being formed rather than the more commonly dominant linear $Rh(NO^+)$ species. DRIFTS also indicates that a second reaction is possible. This becomes increasingly significant for $Rh(CO)_2Cl\{O-Al\}$ samples exposed to air for ca. 2−3 days and results in the $\{Al-O\}Rh^I(CO)_2Cl$ species reacting with NO to form a new species displaying adsorptions at 2150−2110 and 1750−1700 cm^{-1}. Once formed, this latter species reacts no further at room temperature under NO. The DRIFTS spectrum of this species is interpreted as being due to $\{Al-O\}Rh(CO)(NO)Cl$ species existing in cis and trans configurations: the isomer with the carbonyl group trans to the Cl ligand being the preferred form at room temperature. The reconversion of the $Rh(NO^-)$ species under CO shows complex temperature dependence. The consumption of the $Rh(NO^-)$ shows only a weak temperature dependence in terms of EDE, but the observed evolution of NO_g shows a strong temperature dependence. The combination of EDE and MS indicates rapid formation of an intermediate species, most likely $\{Al-O\}Rh(CO)(NO)Cl$, which at room temperature converts to the geminal dicarbonyl species slowly. The possible origins of this behavior, and the parameters determining the formation of "linear" and/or "bent" rhodium nitrosyls in support Rh systems are discussed.

Introduction

The ability to determine the parameters (be they structural or kinetic) that characterize change in chemical systems is highly prized in many areas of chemical investigation. Ideally, such determinations should be made simultaneously, and in well-defined circumstances; from a catalytic point of view these circumstances should, as closely as possible, mirror those that might apply in a larger scale applied situation. Unfortunately, the application of a single technique to a given problem rarely meets these requirements and methods for combining methodologies that yield complementary information on comparable time scales are necessary.

In the study of heterogeneous systems a variety of combined, time-resolved methods, have been demonstrated: for instance, time-resolved EXAFS in both quick EXAFS and energy dispersive (EDE) modes have been successfully combined with X-ray diffraction (XRD).[1−3] Further, our own group,[4−6] along with others,[7,8] have shown that a combination of EDE and MS can yield significant information regarding the relationship between local surface structure and the progress of a given reaction in a dynamic manner on a time scale of a few seconds.

In direct relation to our current area of investigation, the interaction of $Rh^I(CO)_2$ species supported upon TiO_2 and Al_2O_3, with NO, CO, and O_2 has been much studied, using infrared and mass spectrometric based approaches, within the more general investigation of CO oxidation and NO_x removal catalysis over supported Rh systems.[9−22] These have delineated much of the detail of these interactions, which are fundamental to the comprehension of how the component molecules interact and contribute to the overall performance of such catalysts for a given process. However, none of the above has yielded explicit local structure determination on the time scale of the reactions under study, save for those models of local coordination that may be derived from assessment of the position and relative intensities of adsorption bands observed in IR spectra.

Again, in the current case, this is important. It has been amply demonstrated[6,9−26] that the exposure of low-loaded supported

* Corresponding authors. E-mail: m.a.newton@soton.ac.uk, je@soton.ac.uk. Tel: +44(0) 2380 596 744. Fax: + 44 (0) 2380 593 781.
† University of Southampton.
‡ CLRC Daresbury.
§ European Synchrotron Radiation Facility.

10.1021/jp013749k CCC: $22.00
Published on Web 03/30/2002

Rh catalysts to CO and NO can lead to oxidative disruption of small Rh particles and the formation of a variety of Rh species. These species may interact with gas-phase molecules and interconvert in a variety of ways that may or may not be deleterious to the facility of, for instance, NO_x conversion. Species such as $Rh(CO)_2$, $Rh(NO^+)$, Rh(NCO), Rh(CO)(NO), $Rh(NO)_2$, and two forms of $Rh(NO^-)$ have all been identified.[9−22] However, an assessment of the structural and kinetic characters of the various of processes possible in these systems is generally absent.

Most salient in the current case is the existence of two types of $Rh(NO^-)$ species: "high" (∼1750 cm^{-1}) and "low" wavenumber (∼1640 cm^{-1}).[9−22] Vibrational spectroscopic studies on both Rh single crystals[27−29] and high-area systems have been used to infer that the low-wavenumber species exists upon Rh^0 particles and is most likely the intermediate that leads to NO dissociation and, therefore, the conversion of noxious NO to N_2. Similarly, the high-wavenumber NO^- species has been inferred to be bound to isolated Rh atoms adsorbed on the surface[17] though the ramifications of the formation of this species, in terms of for instance de NO_x chemistry are unresolved.

We have recently demonstrated that in situ EDE measurements may be successfully made on powder samples without recourse to pressing.[4−6,30,31] Further, our methodology has been shown to result in data that may be explicitly analyzed for structural information after only a few seconds acquisition. Through interfacing of the microreactor to a mass spectrometer, we may follow the conversion of surface species on time scales of a few seconds and be able to assess the changes in local structure and gas phase composition simultaneously during a reaction. In this paper we expand upon the results shown in a recent communication[4] and use the EDE/MS methodology to investigate the structures, mechanistics, and kinetic character of the reversible conversion of γ-Al_2O_3-supported $Rh^I(CO)_2Cl$ (**I**) to a monodisperse Rh nitrosyl species displaying a bent RhNO bond, i.e., $Rh(NO)^-$ (**II**). We also discuss possible reasons for the formation of linear and/or bent nitrosyls in supported Rh systems.

Experimental Section

Supported $Rh^I(CO)_2/\gamma Al_2O_3$ samples were prepared by first drying the Al_2O_3 in a He flow at 493 K for 6 h; under these conditions the Al_2O_3 is dried but not extensively dehydroxylated.[32] The prepared γ-Al_2O_3 (surface area ca. 100 $m^2\ g^{-1}$) was then placed under vacuum in the presence of a $[Rh(CO)_2Cl]_2$ held at ∼323 K. Under these conditions the $[Rh(CO)_2Cl]_2$ was sublimed onto the γ-Al_2O_3 to produce a yellow powder (ca. 5 wt % Rh). This was then transferred under an inert atmosphere (He) into a sealed Schlenk tube and then kept refrigerated until use. TiO_2 (Degussa P25)-supported samples were produced in an identical manner.

For DRIFTS experiments the samples were transferred to a sample cup that was immediately placed into a sealed DRIFTS cell under constant He purge. The gas flow was changed to CO for ca. 15 min before returning the cell to the He purge. IR spectra were taken using a Perkin-Elmer 1710 spectrometer. At 4 cm^{-1} resolution 100 scans took ca. 600 s. After purging with He, flows of CO or NO (5 mL min^{-1}, 5% NO/He, 5% CO/He) could be switched in and out as necessary.

Sample presentation for the EDE experiment involved the packing of ∼10 mg of the sieved (75−120 mm fraction) supported sample into quartz tubes of ∼2.5 mm i.d. The resulting bed (∼5 mm length) was held in place using quartz wool plugs. The quartz tubes were then placed into a microreactor and subjected to a flow (5 mL/min 5% He/CO) for 15−20 min prior to purging with He.

The microreactor comprises an oven heated by 12 cartridge heaters controlled by a Eurotherm control unit; this oven is punctuated with 10 mm × 3 mm slits that allow the X-ray light to pass through the sample bed. The loaded tubes are placed into this oven and secured at each end using push-on fittings (Linkham Scientific). The reactor configuration allows for two tubes to be held in parallel and experiencing the same gas flows and temperatures. Usually, one tube will be packed with an $I_{(o)}$ containing the unloaded support material. However, it has been empirically found that, at the very high X-ray energies used at the Rh K edge, the addition of this second tube was unnecessary and that air alone acted as an excellent $I_{(o)}$. A Rh foil was held in a third slit and used *for in situ* energy calibration.

The gas flow over the sample could be switched remotely between three feed gases (He, CO/He, and NO/He) and the changes in the post-bed gas composition could be monitored using a Balzers mass spectrometer station interfaced to the reactor exhaust by a 1 m long packed silica column. Under this arrangement the gas flow into the mass spectrometer is kept constant.

In a typical experiment the sample (under He) was brought to the specified temperature and the mass spectrometer and EDE measurements commenced. At a given time after this the gas flow was remotely switched from He to either CO or NO.

The EDE experiments were performed at ID 24 at the ESRF Grenoble, France, using an asymmetrically cut (6°) Si[111] in a Laue geometry.[33,34] Detection in EDE was made using a masked Peltier cooled CCD detector (Princeton). The time resolution of the experiments using this configuration is limited by the data readout time of the detector. As such, though individual spectra are acquired in only 1−2 s, sequential spectra were taken every 4−8 s.

Results

1. DRIFTS Studies. *(a) Reaction of "Fresh" $RhI(CO)_2Cl/Al_2O_3$ with NO.* Figure 1 shows the results of exposing a fresh $Rh^I(CO)_2Cl/Al_2O_3$ sample to NO at room temperature (a) along with (b) a DRIFTS spectrum of the starting geminal dicarbonyl species. The inset plots the integrated intensities of the bands appearing and disappearing during this process. In this case the spectrum of the supported $Rh(CO)_2Cl$ species, supported upon hydroxylated Al_2O_3, has been taken as the background for this experiment before subsequent exposure to doses of 5% NO/He. The consumption of the geminal species is therefore observed in the appearance of positive bands in the region 2110−2030 cm^{-1}; as this sample is exposed to NO, these bands are indeed evident, and concurrently an adsorption band in the region 1700−1760 cm^{-1} evolves. This latter band is indicative of the formation of a species that has been previously observed in similar systems and assigned as being due to the formation of a "high-wavenumber" $Rh(NO^-)$ species. Alongside these changes a minor adsorption is also observed at ca. 2150 cm^{-1}.

This experiment confirms our recent conclusion,[4] derived from explicit analysis of EXAFS data taken with ca. 2 s acquisition time, that the majority product of the reaction "fresh" $Rh(CO)_2Cl$ supported upon hydroxylated Al_2O_3 is a bent, Rh nitrosyl species, and that we may directly associate the structural determinations we have made for this species with the often observed "high-wavenumber NO^-".[9−22] This species is indeed monodisperse (showing no Rh−Rh interactions).

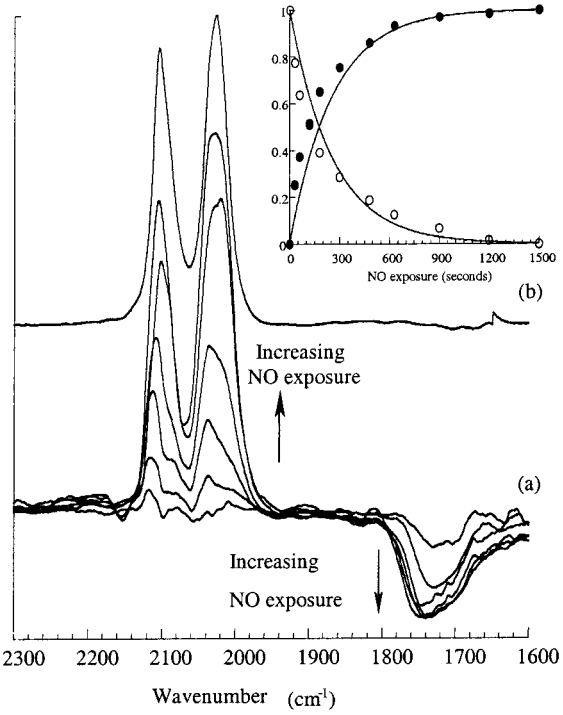

Figure 1. (a) DRIFTS difference spectra during exposure of a fresh $Rh^{I}(CO)_2Cl/Al_2O_3$ (**1**) sample to increasing amounts of NO at room temperature. The removal of surface species is recorded in positive bands, formation in adsorption bands. The inset shows net conversion of the geminal dicarbonyl (open circles) and formation of the nitrosyl as a function of cumulative NO exposure; the solid lines are derived from the kinetic model of this process derived previously.[4] The starting spectrum derived from the fresh $Rh^{I}(CO)_2Cl$ species, and used as the initial background for derivation of the difference spectra, is shown for reference (b).

Though these DRIFTS experiments do not characterize the overall character of the reaction in the same kinetic detail as the previous EDE/MS experiments[4] and are too slow to identify the presence of the [Rh(NO)$_2$Cl]species (ν(NO) at ~1750 and 1830 cm^{-1} [12]) inferred as the reaction intermediate by our previous measurements, the dependence of the measured absorbances in DRIFTS (Figure 1, inset) upon NO exposure is consistent with the pattern of behavior derived from EDE. Further, it can be seen, especially in the early stages of the reaction, that the $Rh^{I}(CO)_2$ species that most readily react with NO are those at the highest wavenumber end of the respective carbonyl absorptions and that the resultant NO adsorption produced from these reactions are at the low-wavenumber (ca. 1720 cm^{-1}) end of the evolving nitrosyl stretch. Previous studies on analogous systems[22,23] have shown only a minimal (if any) blue shifting of the carbonyl species as a function of coverage. Therefore, as this effect is seen in both the symmetric and antisymmetric carbonyl stretches, this reflects the heterogeneity of the Al_2O_3 surface resulting in a distribution of $Rh^{I}-CO$ bond strengths. Those sites displaying the weaker $Rh^{I}-CO$ bonds react most readily and result in the lowest wavenumber (strongest Rh−NO bond) adsorption in the 1720−1760 cm^{-1} region.

(b) Reaction of $Rh^{I}(CO)_2Cl/Al_2O_3$ Samples Exposed to Air, with NO. Figure 2 shows DRIFTS spectra obtained from the exposure of Rh(CO)$_2$Cl/Al_2O_3 samples from the same batch, but after exposure to air for 3 days; as in Figure 1, the inset shows the change in integrated adsorption intensity during exposure for the ν_{asym} of the geminal species (2028 cm^{-1}) and the band at ca. 1745 cm^{-1}. As can be seen after exposure to CO, this sample initially displays a carbonyl infrared signature

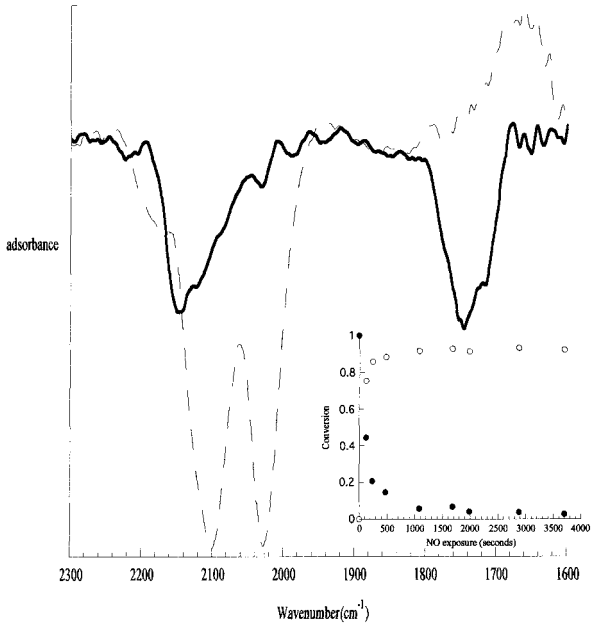

Figure 2. DRIFTS difference spectra recorded before and after exposure of a $Rh^{I}(CO)_2Cl/Al_2O_3$ sample, previously exposed to air at room temperature for 3 days, to NO. The dashed line is that due to the starting geminal dicarbonyl species after room-temperature exposure to CO; the solid line; that derived after exposure to NO. The inset shows net conversion of the $Rh^{I}(CO)_2Cl$ species (from ν_{asymm}(CO) (2028 cm^{-1}) and formation of the nitrosyl band (1745 cm^{-1}) as a function of cumulative NO exposure. In this case the background for derivation of the difference spectra was unloaded Al_2O_3, hence the absence of positive bands due to reactant consumption.

very similar to that derived from the "fresh" sample though an additional high-wavenumber shoulder (at ca. 2180 cm^{-1}) is also observed. The positive band at 1600−1650 cm^{-1} is due to the removal of adsorbed carbonate moieties.[20]

Despite the net similarity in DRIFTS between this supported $Rh^{I}(CO)_2Cl$ species and the "fresh" sample, its reaction with NO at room temperature is very different, resulting in the formation of a new carbonyl band at 2150 cm^{-1} (which shows a considerable asymmetry toward low wavenumbers), and a nitrosyl band centered around 1745 cm^{-1}. For reasons discussed below we assign these feature as due to a {Al−}RhCl(CO)-(NO) species.

(c) Regeneration of $Rh^{I}(CO)_2Cl/Al_2O_3$ Samples from Fresh Samples Initally Reacted with NO. Figure 3 shows DRIFTS spectra, and integrated spectral intensities (inset) charting the reaction of **II** (derived in Figure 1 from the fresh geminal dicarbonyl (**I**)), with CO at room temperature. It is evident that the exposure of CO to this species results in the eventual re-formation of the supported $Rh^{I}(CO)_2Cl$ species though even after considerable exposure to CO the positive band expected from the consumption of the $Rh(NO)^{-}$ species (**II**) indicates an incomplete reaction: the band produced shows only half the expected width of the band due to the $Rh(NO)^{-}$ corresponding to the apparent loss of only the highest wavenumber components of this band at >1750 cm^{-1}.

The progress of the reaction is kinetically very different from the previous two cases, the inset showing that, after a rapid recovery of ca. 25% of the $Rh^{I}(CO)_2Cl$, the reaction slows considerably and takes on the characteristics of a process governed by zero-order kinetics. Moreover, during this slow, apparently constant re-formation of the $Rh^{I}(CO)_2Cl$ species, there is a marked deficit in the apparent level of $Rh(NO)^{-}$ conversion compared to the level of regeneration of the geminal

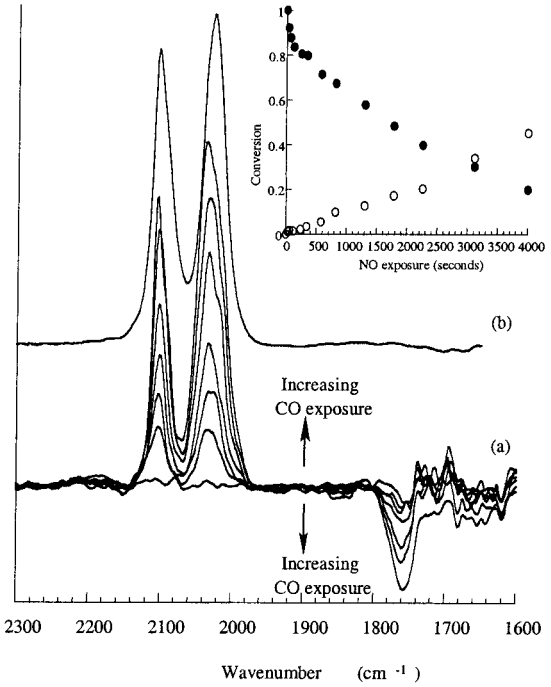

Figure 3. (a) DRIFTS difference spectra obtained from the exposure of the NO treated sample shown in Figure 1 to CO at room temperature. In this case consumption of surface species is registered by (negative) adsorption bands; formation by positive bands. The inset shows the net regeneration of the geminal species (open circles) and apparent comsumption of the nitrosyl species (filled circles). The starting spectrum derived from the fresh $Rh^I(CO)_2Cl$ species under He is also shown for reference (b).

dicarbonyl. This imbalance can be explained if alongside the $Rh(NO^-)$ and $Rh^I(CO)_2Cl$ species another, intermediate, species is formed during the reaction which shows a nitrosyl stretch that overlaps with, and therefore masks the consumption of the lower wavenumber components of the $Rh(NO^-)$ species.

2. EDE/MS Studies of the Regeneration of $Rh^I(CO)_2Cl/Al_2O_3$ Species from "Fresh" Samples Previously Reacted with NO. The regeneration reaction has also been studied using microreactor-based combined EDE/mass spectrometry methodology[4−6,30,31] in a manner similar to that which has already been applied to the reaction of the "fresh" $Rh^I(CO)_2Cl$ species with NO.[4]

Figure 4 shows the dispersive EXAFS results obtained in a typical experiment; the starting point for this run was a completed reaction of **I** with NO. At $t = 0$ the EXAFS signature obtained is that which has been previously analyzed explicitly from EDEXAFS as **II**.[4] As the gas flow is switched from He to 5% He/CO (@ ca. 100 s) the XAFS progressively changes and starts to show a signature that is indicative of a species showing a local Rh environment very similar to that obtained from **I**.

Figure 5 shows the temporal variations observed in intensity of the "white line" at 298, 328, and 349 K; the same approach can be used for the EXAFS feature that appears as the reaction proceeds (Figure 4). This measurement reflects the extent of reaction of the supported $Rh(NO)^-$ species and indicates, in terms of EXAFS, an approximately first-order process showing only a weak dependence upon sample temperature

Figure 6a shows representative k^3-weighted EXAFS derived from (i) the $Rh(NO)^-$ species, and (ii) that derived from the starting spectrum shown in Figure 4. Figure 6b shows k^3 EDE spectra due to (α) the fresh supported $Rh^I(CO)_2Cl$, (β) spectra derived from the run shown in Figure 4 after 500 s, and (γ) after 1500 s exposure to CO. Clearly the k^3 EXAFS derived

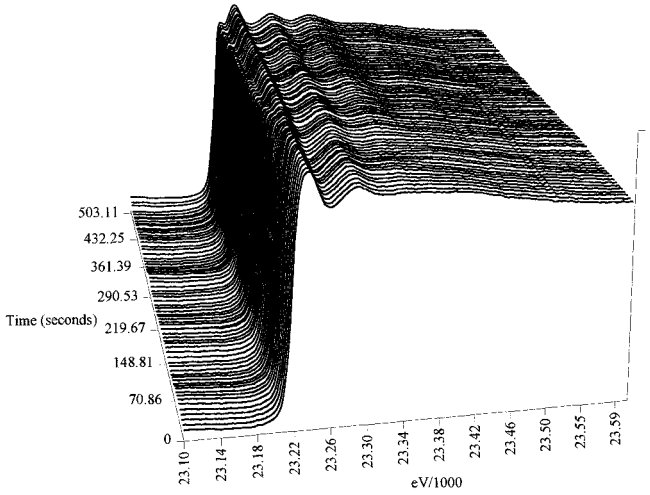

Figure 4. Rh K edge EDE spectra derived during the exposure of a fresh γ-Al_2O_3-supported $Rh^I(CO)_2Cl$ previously reacted with 4% NO/He, to 4% He/CO (5 mL min^{-1}, 3 bar). The switch from a He feed to a CO feed occurs as ca. 100 s. Each spectrum is acquired in ca. 2 s.

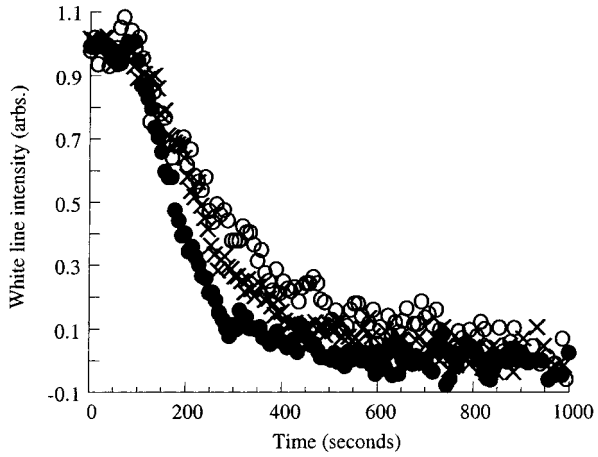

Figure 5. Variation in white line intensity during the switching of gas feed from He to He/CO over species **II** at 298 K (open circles), 328 K (crosses), and 349 K (filled circles).

from the starting species during the regeneration of the $Rh^I(CO)_2Cl$ species from species **I**, is very similar to that which we have previously analyzed. Moreover, spectrum **[γ]**, taken at the end of the CO experiment at ca. 1500 s after the switch to a CO feed is, within the intrinsic noise level of the experiment, identical with that derived from the initial supported $Rh^I(CO)_2Cl$ (species **I**), consistent with the DRIFTS data. However, as indicated from Figure 5, the spectrum derived after ca. 500 s (β) is also essentially identical with that derived from **I**.

The local order around the Rh centers, reflected by the EDE experiments, and initially characteristic of the species **II** changes relatively rapidly, to a species also apparently identical (within the limits of the experimental data) to species **I**, in stark contrast the room-temperature DRIFTS experiments pertaining to this reaction.

Figure 7 shows the new information that emerges from the mass spectral data obtained simultaneously with the EDE: Figure 7a showing the temperature dependence of the production of NO during this reaction; and, Figure 7b the CO response obtained during the experiments together with a blank response obtained from a gas switching experiment made over a bed composed of Rh free Al_2O_3. The inset shows the difference between the experimental spectra and the blank response and may be used to determine net CO uptake. Other masses, for

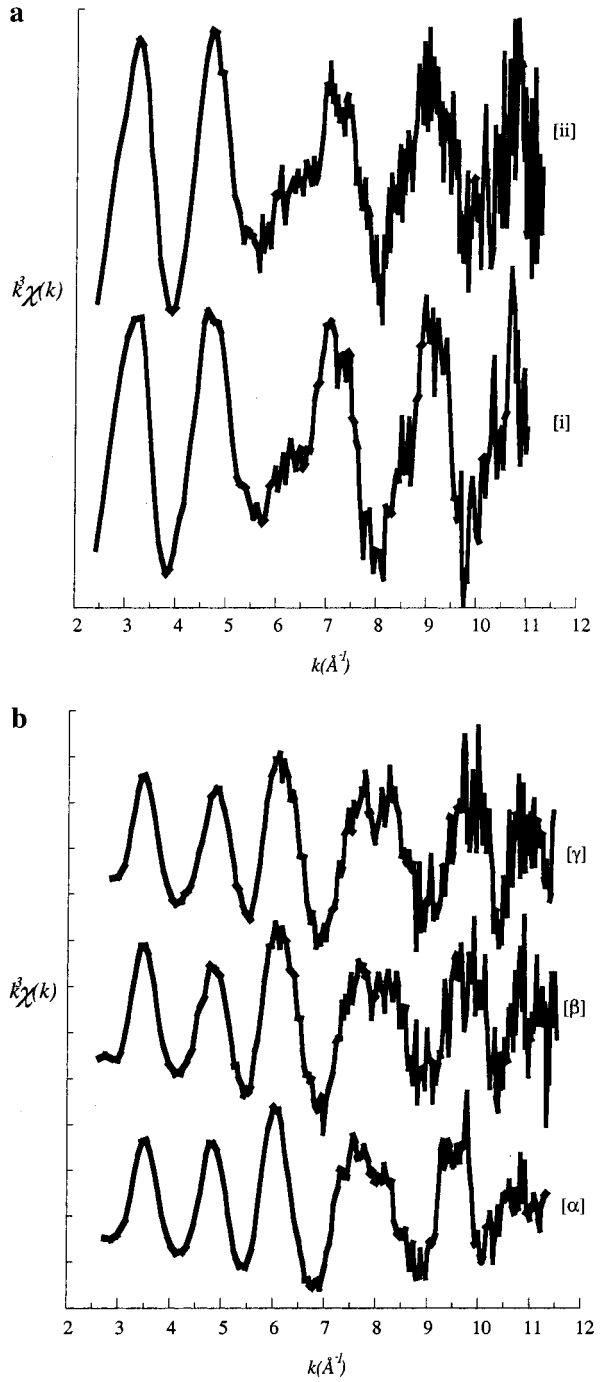

Figure 6. (a) k^3-weighted EDE spectra derived from (i) the bent nitrosyl (species **II**) derived from the reaction of the fresh γ-Al_2O_3-supported $Rh(CO)_2Cl$ species with NO and analyzed explicitly for structural information in ref 4 and (ii) EDE spectrum derived from the starting species prior to exposure to CO at room temperature. In each case the spectra were acquired in ca. 2 s. (b) k^3-weighted EDE spectra derived from (α) the fresh γ-Al_2O_3-supported species **I**, for which explicit structural analysis has previously been presented,[4] (β) the EDE spectrum derived ca. 500 s after switching of the gas feed from He to He/CO, and (γ) the spectrum observed after ca. 1500 s. Exposure to He/CO. Spectral acquisition times are ca. 2 s in each case.

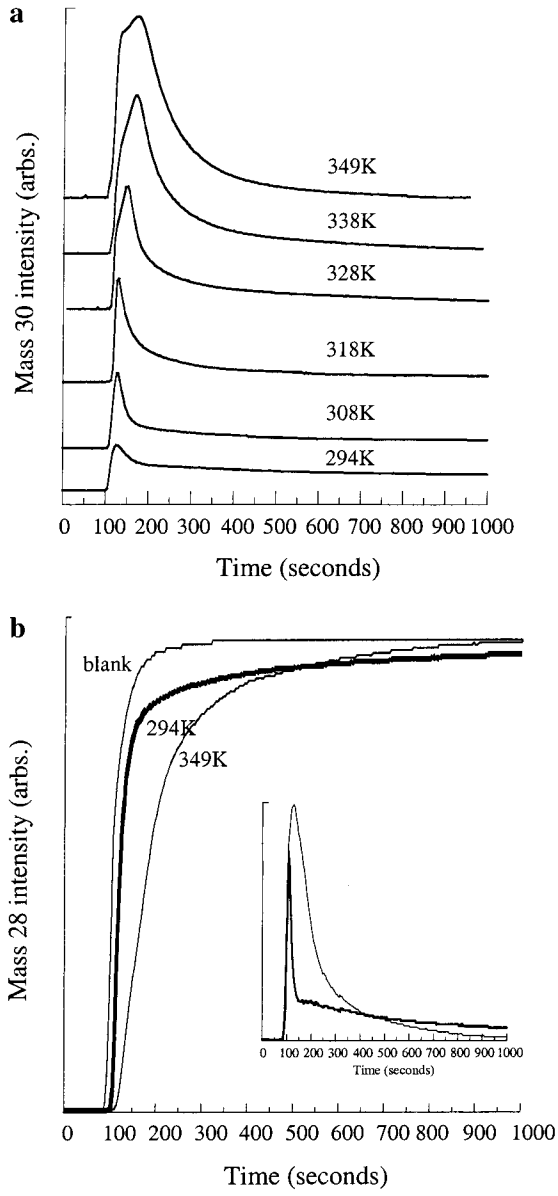

Figure 7. (a) Mass 30 evolution observed during exposure of samples, previously treated with NO (to yield **II**), to CO at the temperatures indicated. The thick line corresponds to the 294 K reaction. (b) Mass 28 responses observed during exposure species **II**, to CO at 298 and 349 K along with a blank response derived from an unloaded Al_2O_3. The inset shows the difference between experimental responses and the blank. Again, the thick line corresponds to the 294 K reaction.

instance $H_2O(18)$, CN(26), CNO(42), and $NO_2(46)$ (not shown) show no significant response during this reaction; some mass 44 evolution (CO_2/N_2O) is observed during CO exposure but the levels at which it appears are not significant in terms of the overall reaction.

These traces show that a strong temperature dependence in the character of the CO uptake and NO evolution in the reaction of **II** with CO. At the lowest temperature investigated, there is an initial, small, burst of NO that decays to a constant level: this (differential) response is entirely consistent with the (integral) character of the reaction derived from DRIFTS (Figure 3 inset). However, whereas after 500 s EDE indicates a local structure and net symmetry, very close to that due to the geminal dicarbonyl (species **I**), both the net CO uptake and NO evolution measurements show that this cannot have been formed in any significant amount.

As the temperature is increased, the initial burst of NO production increases in magnitude until at the highest temperature investigated the NO response rises rapidly and then falls to zero rather than showing a constant nonzero response. The implication of this is that there are two processes that may lead to reaction of **II** with CO. The first shows apparent zero-order character and dominates at room temperature; the second, is a

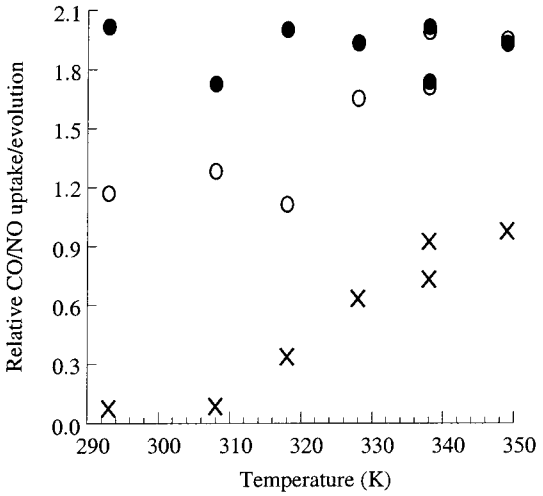

Figure 8. CO uptake (open circles) and NO evolution (crosses) as a function of reaction temperature derived from the mass spectrometer responses shown in Figure 7, and expressed as terms of atoms per Rh atom. Also shown is the total CO production observed during the reaction of **I** with NO (filled circles).

higher order process that increasingly dominates as the reaction temperature is increased.

The apparent conflict between measurement techniques, one reflecting local structure change around the Rh, the other indicating changes in gas-phase composition, is indicative of the formation of an intermediate species with a local Rh environment very similar to the final product, just as was found to be the case of the reaction of **I** with NO to yield species **II**.[4]

Further, though not shown here, analogous systems supported upon hydroxylated TiO_2 show exactly the same reactivity in DRIFTS, resulting in, for instance, the formation of a single ca. 1745 cm^{-1}, "bent NO^-" band from the interaction of the supported geminal dicarbonyl. This is in stark contrast to the behavior observed on both vacuum reduced TiO_2[110] and high-area samples.[22]

Figure 8 shows that results of integrating the spectra of the type shown in the inset to Figure 7, along with the results of integrating the CO evolution profile derived from the in situ EDE/MS studies of the reaction of the supported $Rh^I(CO)_2Cl$ species with NO presented in,[4] as a function of reaction temperature. These show that the apparent uptake of CO at high temperatures equates to the CO evolution observed in the forward experiment indicating that, within the error of the measurements, the same level of CO is evolved and this is a predominantly reversible reaction.

Discussion

(a) Reaction of "Fresh" $Rh^I(CO)_2Cl/Al_2O_3$ with NO. The application of DRIFTS to the reaction of the MOCVD derived $Rh^I(CO)_2Cl$ species supported upon hydroxylated γ-Al_2O_3 verifies the net kinetic character of this process and that the majority product of this interaction is a Rh nitrosyl characterized by a ν(NO) of ~1750 cm^{-1}. Further, the structural determinations afforded by EDE can be associated with the vibrational information provided by infrared spectroscopy, showing the "high-wavenumber" Rh(NO^-) species often observed in studies of supported Rh catalysts as species **II**. The net reaction mechanism, proposed with reference to similar known homogeneous orgno-rhodium chemistry,[35] is shown in Scheme 2.

First, to satisfy a stable, 16-electron count in species **I**, the linkage to the support needs to be of two-electron Lewis base nature and is therefore formalized as involving a hydroxyl

SCHEME 1: Structures of the Supported γ-Al_2O_3-Supported $Rh^I(CO)_2Cl$ Species (I), and "Bent" Rh(NO^-) Species (II) Derived from the Interaction of I with NO_g,Derived from Explicit Analysis of EDEXAFS Data Presented in Ref 4

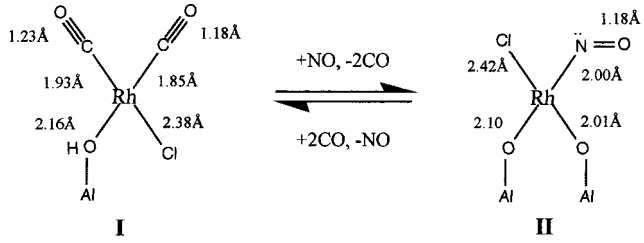

SCHEME 2: Mechanism for the Interaction of "Fresh" γ-Al_2O_3-Supported $Rh^I(CO)_2Cl$ Species (I) with NO_g, Derived on the Basis of Simultaneous EDE/MS Experiments[4]

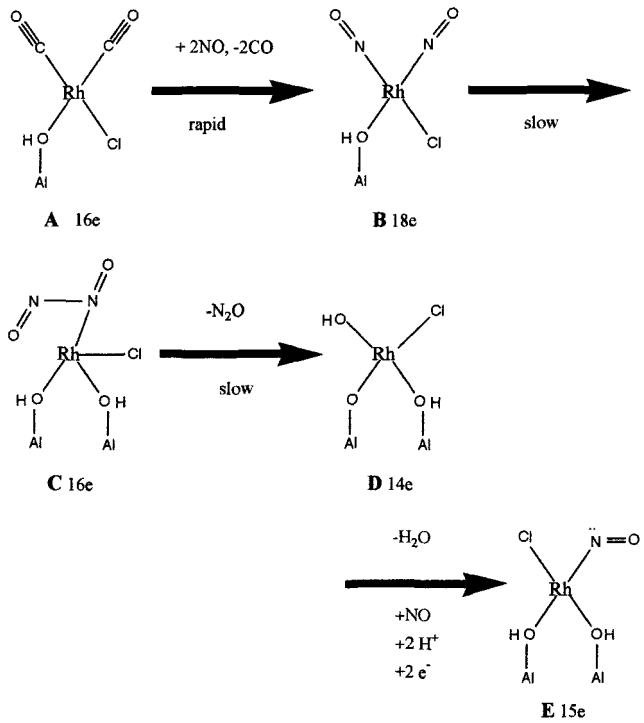

species. Indeed, throughout the reaction scheme the participation of protons appears to be required up to and including the formation of species **II**, where two hydroxyl linkages are required to yield a 15-electron Rh center. While unusual, the production of a relatively stable 15-electron species is not unknown in the chemistry of Rh^{II}.[36] Further, π donation from the Al−O ligands may also occur, as a source of additional stabilization for the Rh center.

Throughout the mechanism the involvement of protons, in the form of hydroxyl species is found to be required to maintain sensible electron counts. Scheme 2 requires the participation of 4 surface protons per Rh center. Previous work has indicated that below ca. 770 K Al_2O_3 may retain a surface hydroxylation level of between 8 and 12 OH nm^{-2}.[32] As the Rh loadings used will produce a maximum of ca. 3 Rh centers nm^{-2}, the overall mechanism is potentially viable in this sense, given the possible error in each estimate, and the pretreatment of the Al_2O_3 (to only 493 K) is taken into account.

This mechanism is rate limited by the decomposition of the transiently formed geminal dinitrosyl species (involving an N_2O_2 ligand) and **C** illustrates the rate-limiting step that involves both

a rehybridization of one of the NO centers and a N−N bond rotation. This brings the terminal O from one of the NO groups into the correct configuration to react with the Rh center and would be consistent with the magnitude of the preexponential factor obtained for this reaction from kinetic analysis.[4]

Further, the proposed mechanism accounts for the simultaneous production of NO and H_2O observed in this reaction by mass spectrometry;[4] although these species appear in differing steps in the reaction sequence, the reaction of species **D** to yield a very reactive 14-electron center **(E)** will mean that in practice both NO and H_2O will appear together.

However, this reactivity only applies to "fresh" samples. DRIFTS studies made using samples exposed to air for 2−3 days at room temperature show a considerably different reactivity.

(b) Reaction of $Rh^I(CO)_2Cl/Al_2O_3$ Samples Exposed to Air, with NO. After exposure to CO a broad positive band (due to removal of surface carbonates) is observed at ca. 1650 cm^{-1} along with the carbonyl stretches due to **I**. As discussed above, the carbonyl spectrum is identical with that derived from the "fresh" sample save for a shoulder at ca. 2180 cm^{-1}. The precise origin of this shoulder is not certain though similar absorptions observed in supported Rh systems have generally been associated with the formation of Rh(NCO).[10,11,14]

Room-temperature exposure of this sample does not result in the formation of **II** but a new species showing both nitrosyl (ca. 1745 cm^{-1}) and carbonyl (ca. 2150 cm^{-1}) stretches. Supported Rh(CO)(NO) species are often observed in supported Rh systems and are generally characterized by ν(CO) ∼ 2100 cm^{-1} and ν(NO) ∼ 1745 cm^{-1}.[9−18,20−22] Therefore at first sight the position of the carbonyl band at the relatively high wavenumber of 2150 cm^{-1} would mitigate against this species being responsible for the EDE spectra derived during the reaction with CO, as shown in Figure 6b. However, this carbonyl feature is very asymmetric toward lower wavenumbers; it is this that suggests that the species being formed is a supported Al(O)Rh(CO)(NO)Cl species rather than (for instance) being due to predominant formation of NCO and CN species.

While this system has not been investigated using EDE, the EXAFS derived from the other reactions investigated indicates the RhCl bond is consistently retained. As such, the formation of a square-planar Al(O)Rh(CO)(NO)Cl might be expected to result in the formation of two isomers: one with the Cl atom trans to the CO ligand; the other with the Cl cis to the CO (shown as species **III** and **IV**, below).

From a spectroscopic standpoint the effect of the Cl ligand trans to the CO or NO species, rather than the Al(O) species, will be to induce a blue shift in the CO or NO absorption. As such, it would be expected that a square-planar species of this type will give rise to two CO or NO resonances split energetically by the increased electron withdrawing of the Cl over the Al(O) linkage. The intrinsically broad nature of the nitrosyl stretches means that only in the carbonyl region might this effect be observed. However, the distinct asymmetry observed between 2150 and 2100 cm^{-1}, would be consistent with this notion. Therefore we suggest that the IR spectrum observed in Figure 2 is due to the formation of the two isomeric forms of {Al−O}Rh(CO)(NO)Cl (**III** and **IV**), with the majority isomer being that with the CO ligand trans to the Cl (**III**). These isomers are formed very rapidly but once synthesized do not react further with NO. This is in significant contrast to the "fresh" samples, though even in this case, there is evidence for the formation of a very small band at 2150 cm^{-1} (Figure 1).

SCHEME 3: Illustration of Possible Cis ((iii) and Trans (IV) Isomers in Supported (Al−O)Rh(CO)(NO)Cl Species

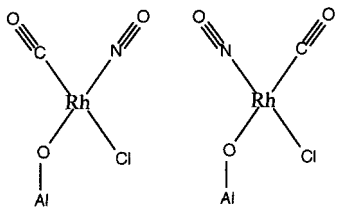

III, trans **IV, *cis***

(c) Regeneration of $Rh^I(CO)_2Cl/Al_2O_3$ Samples from Fresh Samples Initally Reacted with NO. The regeneration of the $Rh^I(CO)_2Cl$ species from the supported {Al−O}RhCl(NO^-) **(II)**, is kinetically very different from the formation of **II** itself**,** being generally much slower and characterized by two distinct regimes: a low-temperature, near zero-order regime that is progressively superseded by more obvious first-order kinetics as the reaction temperature is increased.

The in situ mass spectrometric and DRIFTS analyses both show that, at room temperature, the rapid local order change observed in EDE cannot be due to the re-formation of a majority species **I**; even after considerable exposure to CO the intensities of the IR bands due to the geminal dicarbonyl only indicate ca. 80−85% regeneration. Moreover, in DRIFTS an apparently incomplete loss of **II** is observed with only a narrow high-wavenumber end of the stretch due to this species being observable as being reacted. The apparent deficit in the level of conversion of **II** compared to the formation of the geminal species (inset Figure 3), along with the local order changes observed in EDE clearly point to rapid formation of an intermediate species having a local Rh coordination sphere that is very similar to **I**. Analysis of CO uptake and NO production at low reaction temperatures formulates the intermediate involved as being {Al−O}Rh(CO)(NO)Cl (**III** and/or **IV**). From the arguments presented above regarding the reactivity of the supported $Rh^I(CO)_2Cl$ system exposed to air for a considerable length of time, the formation of this species should result in the appearance of ν(CO) and ν(NO) stretches in the region of 2150−2110 and ca. 1745 cm^{-1}. The DRIFTS obtained during the reaction with CO are not conclusive in regard to the presence of the carbonyl stretch due to the hypothetical Al(O)Rh(CO)-(NO)Cl species, though a residual adsorption can be detected at ca. 2150 cm^{-1}. The nitrosyl region of the infrared spectrum, however, provides indirect evidence that a band is persisting that masks the true level of the conversion of **II**. Further, from the position of the NO band observed in Figure 2 (and associated with an (Al−O)Rh(CO)(NO)Cl species), the presence of such a feature during the reaction with CO would effectively cancel out a considerable (low wavenumber) proportion of the spectral change anticipated from the loss of the bent nitrosyl

The predominant reaction of the supported Rh(NO^-) species to yield a support geminal dicarbonyl is suggested to proceed as is shown in Scheme 4.

The slow, low-temperature, re-formation of **I** would seem to have two possible origins. The first would require that only certain sites on the Al_2O_3 surface permit subsequent reaction of the species **III** or **IV** to **I**. At the start of an experiment, therefore, a portion of these sites are occupied and react relatively rapidly to yield a geminal dicarbonyl species resulting in the initial, but small, burst of NO observed in the mass spectrometer at lower temperatures. Once this has occurred, any subsequent reaction of the remaining population of (Al−O)-Rh(CO)(NO)Cl species would require the migration of the

SCHEME 4: Mechanism for the Reaction of the Bent, Monodisperse, Rh(NO−) Species with CO_g Derived from Simultaneous EDE/MS Measurements and from DRIFTS

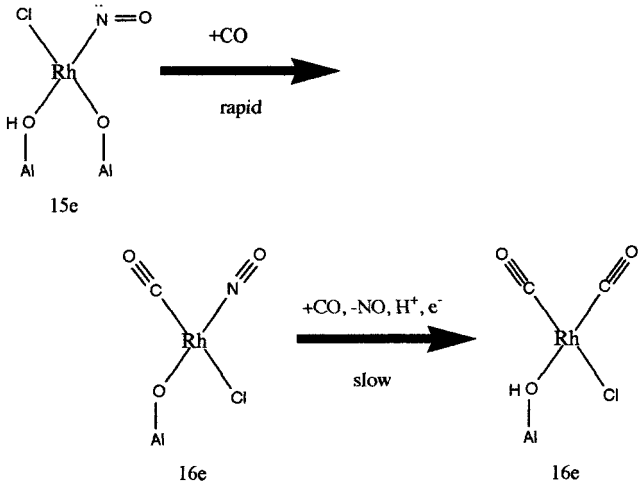

geminal dicarbonyl species away from the reactive sites before any further reaction can be initiated. As such, the rate would become diffusion controlled with a relatively small number of reactive sites controlling the production of the geminal species from a large reservoir of unreactive (Al−O)Rh(CO)(NO)Cl admolecules. Thus the reaction is slow and shows approximately zero order character.

In support of this, scanning tunneling microscopy measurements made upon the analogous $[Rh(CO)_2Cl]_2$-derived geminal dicarbonyl adlayer adsorbed on TiO_2[110] do show that the adsorbed $Rh^I(CO)_2Cl$ species are capable of structural reorganization at room temperature and on similar time scales.[37]

However, there is a second possibility: that the two isomeric forms of the (Al−O)Rh(CO)(NO)Cl intermediate species (**III** and **IV**) exhibit a marked difference in reactivity toward CO. This could arise due to the differential in Rh−N bond strengths caused by the NO being bonded in a cis or trans manner relative to the Cl species. The trans configuration **III** the Rh−N bond will be weakened due to the relative diminution of back-bonding from the Rh compared to the cis case **IV** where the NO ligand exists trans to the Al−O linkage.

In terms of infrared the NO trans to the Cl will contribute a blue-shifted component to the ν(NO) adsorption and a red-shifted component to the ν(CO) region of the spectrum. The alternate cis configuration will result in a relatively blue-shifted carbonyl stretch and a red-shifted ν(NO).

From the bond strength arguments made above the cis form **IV** of the Al(O)Rh(CO)(NO)Cl will contain the most tightly bound NO ligand and, therefore, hypothetically the less reactive toward ligand substitution to yield the $Rh^I(CO)_2Cl$ species. If the rate of removal of **IV** to form the species **I** is rapid enough, the net rate of formation of the geminal species at low temperatures will be predominantly controlled by the equilibrium between cis and trans isomers. This would result in a slow rate of reaction that could result in apparent zero-order kinetics.

This mechanism implies that a degree of the differential in Rh−N bond strengths resulting from a cis or trans configuration is expressed in the reaction transition state. This would therefore indicate a degree of dissociative character rather than the predominantly associative kinetics observed in ligand exchange reactions in solution phase square-planar complexes.[38] However, the analogous (solution phase) and associative exchange between CO_g and CO ligands in the related family of *cis*-$[Rh(CO)_2X_2]^-$ (X = Cl, Br, I)[39] also shows a considerable trans influence with the obtained rate of exchange varying as Cl < Br < I (1:15:525), with ca. 80% of the change in rates between chloro and bromo analogues being accounted for purely by the change in reaction enthalpy between systems. Indeed, all other parameters being equal and in the absence of significant steric effects, a bond strength differential of as little as 5.7 kJ mol^{-1} would result in the (Al−O)Rh(CO)(NO)Cl trans isomer being 10 times as reactive as the cis. As such, we cannot reasonably rule this mechanism out as the source of the observed low-temperature kinetics.

Having established the kinetic character of both forward and reverse reactions of the supported geminal species under NO and then CO, and the structures of the major species involved, we ask why the nitrosyl formed in this case is a "high-wavenumber" $Rh(NO^-)$ species rather than, for instance, the more commonly observed linear $Rh(NO^+)$ species.

The mechanism shown in Scheme 4 clearly requires the presence of a relatively high degree of surface hydroxylation. Further, as noted above, TiO_2 samples treated in a similar manner, i.e., to retain a high degree of hydroxylation, react in an identical manner to that shown here for hydroxylated Al_2O_3-based systems. This is in stark contrast to the recently determined reactivity of the $Rh^I(CO)_2Cl$ species derived from the same $[Rh^I(CO)_2Cl]_2$ precursor on vacuum-reduced single-crystal ([110] oriented) and powder TiO_2.[22] In these cases the dominant product of the reaction of the geminal dicarbonyl species is found to be the linear $RhNO^+$ species.

A clear implication of these results is that the level of support hydroxylation is crucial in determining how species such as the supported geminal dicarbonyl species react with NO: their presence promoting the formation of a bent nitrosyl configuration; their absence forcing the adoption of a linear RhNO system.

More generally, typical preparations of supported Rh catalysts involve calcinations and reduction procedures at elevated (573−773 K) that will result in variable lower levels of hydroxyl retention by the support than produced here. As such, we should expect that in general the formation of linear nitrosyls from geminal dicarbonyl species should be generally preferred, and indeed, this has been generally found to be the case.

A notable exception is the behvior of Rh catalysts supported upon SiO_2 where high (ca. 5 wt %)[18] Rh loadings lead to the majority formation of a linear nitrosyl after reaction with NO, whereas loadings of Rh at the 0.5% level[17] result in a majority bent NO species of the type observed in the current studies. Hydroxylated SiO_2 only yields a maximum OH density of ca. 4−5 OH nm^{-2}.[32,40] As such, if the same general principles apply, it is clear that at 5 wt % loading there may not be enough surface protons available to support a significant level of bent nitrosyl formation and, therefore, once again the formation of $Rh(NO^+)$ will dominate. However, when the Rh loading is decreased by a factor of 10, the situation is reversed, with the potential surface hydroxyl level outstripping the Rh atom loading. As such, and as long as the protons are mobile and reactive, the interaction with NO will then lead to the formation of a majority high-wavenumber $Rh(NO)^-$ species, as is observed.

Conclusions

The correlation of in situ combined EDE/MS results with in situ DRIFTS measurements allows the direct association of local structure with vibrational spectroscopic information and indicates the nature of the product of the interaction of $Rh^I(CO)_2Cl$ supported upon hydroxylated γ-Al_2O_3 as a monodisperse, square-planar $Rh(NO)^-$ species (**II**). Further, the derived mech-

anism for this conversion indicates that the formation of the bent nitrosyl, over the more commonly observed linear nitrosyl, requires the participation of a significant number of mobile surface hydroxyl species.

However, and for reasons as yet undetermined, exposure of the $Rh^{I}(CO)_2Cl/\gamma$-Al_2O_3 for prolonged periods to air leads to the reaction following a differing pathway resulting in the formation of a supported Rh(CO)(NO) species which persists under NO in a majority isomeric form with the carbonyl species trans to the electron withdrawing Cl ligand (**III**).

The reaction of the supported $Rh(NO)^-$ species with CO results in re-formation of **I** and proceeds via the initial formation of a Rh(CO)(NO) center. This subsequently reacts to yield the geminal dicarbonyl (**I**). At all temperatures EDE shows the formation of the intermediate species is relatively facile, showing only a weak dependence upon sample temperature. However, both DRIFTS and MS show that the subsequent formation of the geminal dicarbonyl from the Rh(CO)(NO) species is temperature dependent, showing close to zero-order character at lower temperatures. As the reaction temperature increases, this is progressively superseded at increasing temperatures by a more obvious first-order character. At present, though we can postulate that this temperature dependence may have its origins in diffusion-dominating reactivity at lower temperatures, or in reactivity of the *cis*- and *trans*-[Al−O]Rh(CO)(NO)Cl species (**III** and **IV**), differentiation between these possibilities is not currently possible.

Last, from the measurements presented here by others previously published in the literature made on supported Rh systems, we have been able to formulate a qualitative framework within which the reasons for the formation of different ("bent" $Rh(NO^-)$ versus "linear" $Rh(NO^+)$ species) may be understood. Central to this is degree of support hydroxylation. This has to be high relative to the Rh loading to yield significant formation of the monodisperse bent nitrosyl rather than the equivalent linear nitrosyl.

Acknowledgment. This work was funded under the "Catalysis and Chemical Processes" initiative of the EPSRC, and the EPSRC is acknowledged for its funding of a postdoctoral position to M.A.N., and Ph.D. funding to D.G.B., S.G.F., and T.C. (via a CASE award in partnership with BNFL Plc). BP chemicals and the University of Southampton are also thanked for Ph.D. funding to S.T. We also thank the ESRF, Grenoble, France, for access to facilities and to acknowledge Sebastian Pasternak, Ralph Wiegel, Mike Caplin, Melanie Hill, John James, and the late Bruce Hancock, whose technical skills have contributed greatly to the progress of this research.

References and Notes

(1) Couves, J. W.; Thomas, J. M.; Waller, D.; Jones, R. H.; Dent, A. J.; Derbyshire, G. E.; Greaves, G. N. *Nature* **1991**, *354*, 465.
(2) Clausen, B. S.; Topsøe, H.; Frahm, R. *Adv. Catal.* **1998**, *42*, 315.
(3) Molenbroek, A. M.; Norskov, J.; Clausen, B. S. *J. Phys. Chem. B* **2001**, *105*, 5450.
(4) Newton, M. A.; Burnaby, D. G.; Dent, A. J.; Diaz-Moreno, S.; Evans, J.; Fiddy, S. G.; Neisius, T.; Pascarelli, S.; Turin, S. *J. Phys. Chem A* **2001**, *105*, 5965.
(5) Campbell, T.; Dent, A J.; Diaz Moreno, S.; Evans, J.; Fiddy, S G.; Newton, M A.; Turin, S. *Chem Commun*. **2002**, 304.
(6) Newton, M. A.; Dent, A. J.; Diaz-Moreno, S.; Fiddy, S. G., Evans, J. *Angew. Chem., Int. Ed. Engl.*, submitted for publication.
(7) Ressler, T.; Timpe, O.; Neisius, T.; Find, J.; Mestl, G.; Dieterle, M.; Schlögl, R. *J. Catal*. **2000**, *191*, 75.
(8) Ressler, T.; Hagelstein, M.; Hatje, U.; Metz, W. *J. Phys. Chem. B* **1997**, *101*, 6680.
(9) Arai, H.; Tominaga, H. *J. Catal*. **1976**, *43*, 131.
(10) Rasko, J.; Solymosi, F. *J. Catal*. **1981**, *71*, 219.
(11) Hyde, E. A.; Rudham, R. *J. Chem. Soc. Faraday. Trans*. **1984**, *80*, 531.
(12) Liang, J.; Wang, H. P.; Spicer, L. D. *J. Phys. Chem.* **1985**, *1985*, 5840.
(13) Cannon, K. C.; Jo, S. K.; White, J. M. *J. Am. Chem. Soc.* **1989**, *111*, 5064.
(14) Dictor, R. *J. Catal.* **1988**, *109*, 89.
(15) Srinivas, G.; Chuang, S. S. C.; Debnath, S. *J. Catal.* **1994**, *148*, 748.
(16) Krishnamurthy, R.; Chuang, S. S. C. *J. Phys. Chem.* **1995**, *99*, 16727.
(17) Chuang, S. S. C.; Tan, C.-D. *Catal. Today* **1997**, *35*, 369.
(18) Chuang, S. S. C.; Tan, C.−D. *J. Catal.* **1998**, *175*, 95.
(19) Cavers, M.; Davidson, J. M.; Harkness, I. R.; Rees, L. V. C.; McDougall, G. S. *J. Catal.* **1999**, *188*, 426.
(20) Kondarides, D. I.; Chafik, T.; Verykios, X. E. *J. Catal.* **2000**, *190*, 446; *191*, 142.
(21) Almusaiteer, A.; Chuang, S. S. C.; Tan, C−D. *J. Catal.* **2000**, *189*, 247.
(22) Hayden, B. E.; King, A.; Newton, M. A.; Yoshikawa, Y. *J Mol. Catal. A* **2001**, *167*, 33.
(23) Zubkov, T. S.; Wovchko, E. A.; Yates, J. T. *J. Phys. Chem. B* **1999**, *103*, 5300.
(24) Yates, J. T.; Duncan, T. M.; Worley, S. D.; Vaughan, R. W. *J. Chem. Phys.* **1979**, *70*, 1219.
(25) Van't Blik, H. F. K.; Van Zon, J. B. A. D.; Huizinga, T.; Vis, J. C.; Koningsberger, D. C.; Prins, R. *J. Phys. Chem.* **1983**, *87*, 2264.
(26) Johnston, P.; Joyner, R. W. *J. Chem. Soc., Faraday Trans*. **1993**, *89*, 863.
(27) Root, T. W.; Fisher, G. B.; Schmidt, L. D. *J. Chem. Phys.* **1986**, *85*, 4679.
(28) Root, T. W.; Fisher, G. B.; Schmidt, L. D. *J. Chem. Phys*. **1986**, *85*, 4687.
(29) Permana, H.; Ng, K. Y. S.; Peden, C. H. F.; Schmeig, S. J.; Lambert, D. K.; Belton, D. N. *J. Catal*. **1999**, *164*, 194.
(30) Fiddy, S. G.; Newton, M. A.; Dent, A. J.; Salvini, G.; Corker, J. M.; Turin, S.; Campbell, T.; Evans, J. *Chem. Commun.* **1999**, 851.
(31) Fiddy, S. G.; Newton, M. A.; Campbell, T.; Corker, J. M.; Dent, A. J.; Harvey, I.; Salvini.; Turin, S.; Evans, J. *Chem. Commun.* **2001**, 445.
(32) Peri, J. B. *J. Phys. Chem.* **1965**, *69*, 220.
(33) Hagelstein, M.; Ferraro, C.; Hatje, U.; Ressler, T.; Metz, W. *J. Synchrotron Rad*. **1995**, *2*, 174.
(34) San Miguel, A.; Hagelstein, M.; Bornel, J. C.; Marot, G.; Renier, M. *J. Synchrotron Radiation* **1998**, *5*, 1396.
(35) Bhaduri, S.; Johnson, B. F. G.; Savoury, C. J.; Segal, J. A.; Walter, R. H. *J. Chem. Soc., Chem. Commun*. **1975**, 809.
(36) De Wit, D. G. *Coord. Chem. Rev*. **1996**, *147*, 209.
(37) Newton, M. A.; Bennett, R. A.; Smith, R. D.; Bowker, M.; Evans, J. *Chem Commun.* **2000**, 1677.
(38) For instance: Wilkins, R. G. *Kinetics and Mechamism of Reactions of Transition Metal Complexes*; VCH: Weinheim, Germany, 1991.
(39) Churlaud, R.; Frey, U.; Metz, F.; Merbach, A. E. *Inorg. Chem.* **2000**, *39*, 304.
(40) Turin, S.; Evans, J. Unpublished results.